

Monitoring the cellular uptake of Silica-Coated CdSe/ZnS quantum dots by Time lapse Confocal Laser Scanning Microscopy

Heba ElSayed ElZorkany¹, Haidan M. El-Shorbagy², Khaled Yehia Farroh¹, Tareq Youssef³, Salwa Sabet²,
Taher A. Salaheldin^{1,4*}

¹Nanotechnology and Advanced Materials Central Lab, Agricultural Research Center, Egypt.

²Department of Zoology, Faculty of Science, Cairo University, Egypt.

³Department of Photochemistry Photobiology, National Institute for Laser Enhanced Science (NILES), Cairo University, Egypt.

⁴Nanotechnology Research Centre, British University in Egypt.

ARTICLE INFO

Article history:

Received on: 24/08/2017

Accepted on: 28/12/2017

Available online: 30/03/2018

Key words:

Quantum dots, silica coating, confocal microscopy, HepG2 cells, *in vitro* toxicity.

ABSTRACT

In this study, we aimed to investigate the efficiency of silica coated CdSe/ZnS nanocrystals (CdSe/ZnS-SiO₂ NCs) for imaging purposes. CdSe quantum dots (QDs) were synthesized by organometallic routes and were coated with ZnS shell by injecting solutions of diethylzinc (Zn (Et)₂) and hexamethyldisilathiane ((TMS)₂ S) as precursors for zinc and sulfur ions respectively. Then, CdSe/ZnS QDs were rendered water soluble by overcoating with silica using tetraethyl orthosilicate (TEOS) as a silica precursor. QDs were characterized by UV-Vis absorption, emission spectroscopy TEM, XRD and DLS. The biocompatibility of silica-coated QDs (CdSe/ZnS-SiO₂) was tested by evaluating mitochondrial activity of liver hepatocellular carcinoma (HepG2) cells exposed to different concentrations of CdSe/ZnS-SiO₂. CdSe/ZnS-SiO₂ cytotoxicity was evaluated by investigating DNA damage using alkaline comet assay. The intracellular uptake and localization of QDs in HepG2 cells were monitored by fluorescence imaging using Confocal Laser Scanning Microscopy (CLSM) up to eight hours. Results showed that silica coating yielded final particles' size around 35 nm possessing strong luminescence property. The cytotoxicity test results showed that CdSe/ZnS-SiO₂ were nontoxic at low concentrations. CLSM showed that HepG2 cells depicted fast internalization of CdSe/ZnS-SiO₂ into the cells with very good fluorescence emission in the cytoplasmic portion.

INTRODUCTION

Quantum dots (QDs) are zero-dimensional nanoparticles in which charge carriers in the system are confined in all dimensions (Medintz and Hildebrandt, 2014). QDs are a very interesting nanomaterial with unique characteristics, that could help in many clinical and pharmaceutical purposes (Peuschel *et al.*, 2016).

Due to its intrinsic photophysical properties, QDs are promising tools for many biological applications. Recently, QDs have even been tested for multicolor optical barcodes (Kim *et al.*, 2016), visualizing *in vitro* protein movements, microbiological labels, detection of dual DNA targets (Cui *et al.*, 2016). The

optical properties of QDs are much suited to imaging purposes than those of molecular fluorophores (Thomas, 2015). However, organic fluorophores have limited usage in long-term imaging as it has broad absorption/emission profiles in addition to the low photobleaching thresholds (Medintz and Hildebrandt, 2014).

QDs show interesting advantages for lots of applications. They exhibit a high fluorescence yield especially cadmium based QDs. This kind of QDs started to play a role in molecular pathology and malignant-tumor biomarkers (Massey *et al.*, 2015). However, QDs also possess a serious disadvantage manifested in the high toxicity (Oh *et al.*, 2016). Recently, QDs showed distinct cell damage, resulting from ROS receptor generation and lysosome increment inside the cell (Liu *et al.*, 2017), the thing that led researchers to make further surface modifications to them. Most of surface modifications cause a complete or partial loss of photoluminescence (PL) (Hoshino

*Corresponding Author

Taher A. Salaheldin, Mostafa Elsayed Center for Nanotechnology Research, British University in Egypt. E-mail: Taher.salah@bue.edu.eg

et al., 2011). Growing a silica shell around the QDs is a very special type of surface modification, as it doesn't only increase the PL of the QDs but also it becomes biocompatible rather than it enhances the uptake of QDs by biological cells (Dhawan and Sharma, 2010).

In the present study, we have synthesized silica coated CdSe/ZnS nanocrystals (CdSe/ZnS-SiO₂ NCs) that have been tested for imaging purposes. Therefore, the uptake of CdSe/ZnS-SiO₂ inside live HepG2 cells was monitored for eight hours by Confocal Laser Scanning Microscopy (CLSM). The results showed a very fast uptake and stability of the CdSe/ZnS-SiO₂ NCs inside HepG2 cells.

MATERIALS AND METHODS

Chemicals

Ammonium hydroxide (NH₄OH, MW 35.1, 33%) Cadmium oxide (CdO, 99.99%), chloroform 99.7%, diethylzinc (Zn (Et)₂), ethanol (99.9%), hexamethyldisilathiane (TMS)₂S Hexadecylamine (HDA, 98%), Oleic acid (OA, 90%), Polyoxyethylene (5) nonylphenyl ether (Igepal CO-520, Ave. MW 441), Selenium (99.5%, 100 mesh), Tetraethyl orthosilicate (TEOS, 98%), Trioctylphosphine (TOP, 97%), Trioctylphosphine oxide (TOPO, 99% Merck), Sodium Hydroxide (NaOH), Sodium Chloride (NaCl), Water-soluble tetrazolium kit (WST-1, Clontech Laboratories, Takara Co., Japan), low melting point agarose (LMA), Dimethylsulfoxide (DMSO), Disodium EDTA, Ethidium Bromide, Phosphate Buffered Saline (PBS) (Ca⁺⁺, Mg⁺⁺ free), Hanks Balanced Salt Solution (HBSS) (Ca⁺⁺, Mg⁺⁺ free), RPMI-1640 media (Lonza, Belgium). All chemicals were of analytical grade and were purchased from Sigma-Aldrich, unless otherwise was mentioned, and were used directly without further purification. Ultrapure deionized water was obtained from a Milli-Q Synthesis system.

Synthesis of quantum dots

Size-tunable The synthesis of CdSe capped with trioctylphosphine oxide (CdSe-TOPO) nanoparticles QDs was synthesized as previously described (Peng and Peng, 2001). In a typical synthesis, trioctylphosphine selenide was prepared by dissolving 0.15 g Se in 4 mL of TOP, at 200°C in a three-necked flask under N₂ atmosphere until Se is completely dissolved.

In another three-necked, 0.17 g CdO and 2.67 ml oleic acid was ignited to 200-250°C under an argon gas until the red color disappeared. A mixture of 1.94 g TOPO and 1.94 g HDA were added to the reaction vessel, and the temperature was further increased to 300°C. At this temperature, the vessel was removed and trioctylphosphine selenide solution was swiftly inoculated into the reaction mixture under vigorous stirring, which resulted in an instantaneous nucleation and growth of the nanoparticles.

Formation of ZnS shell on CdSe QDs

Formation of ZnS shell on CdSe was applied as previously described (Ibrahim *et al.*, 2014). Typically, in a three-necked flask 0.9 g TOPO and 0.9 g HDA were loaded and heated up to 170°C under magnetic stirring and N₂ gas. Later, CdSe

was added in 1-octadecene solution. Then, a premixed solution containing shell components in 2 ml TOP (1 ml Zn(Et)₂, and 220 µl (TMS)₂S 1.0 M in hexane) was added dropwise into the reaction mixture in a period of 10 min. The reaction mixture was then stirred for one hour at 170°C, then left for cooling. The synthesized CdSe/ZnS NCs were purified and washed by precipitation via the addition of 5:1 ethanol: CdSe/ZnS NCs. The precipitate was collected by centrifugation at 3000 rpm for 5min. The washing process was repeated three times then the precipitate re-dissolved in a minimum amount of chloroform.

Silica coating of QDs

To be suitable for imaging purpose the prepared core/shell QDs should be transferred from organic to aqueous media, so, the prepared hydrophobic ZnS/CdSe were overcoated with Silica-based using the procedure of Vbin *et al.* (Vbin *et al.*, 2014). Typically, a mixture of TOPO capped ZnS/CdSe QDs in 400 µL tetrahydrofuran and 150 µL TEOS was under sonication for 30 min, in an inert atmosphere. This mixture was added to premixed solution of 1 mL Igepal CO-520 in 10 mL cyclohexane and stirred for 30 min. Ammonia solution (1 mL, 33 wt.%) was added dropwise, and the stirring was continued for one day. The CdSe/ZnS-SiO₂ NCs were purified by repeatedly washing with dry propanol, ethanol, and water. Later on, the surface modified hydrophilic CdSe/ZnS-SiO₂ NCs were re-dispersed in sterile PBS for biological evaluation tastes. NCs were stored in the dark at room temperature.

QDs characterization

TEM images, XRD and various spectroscopic and microscopic techniques were employed to characterize morphology, structure, crystallinity, size, absorption and emission of the prepared CdSe, CdSe/ZnS and CdSe/ZnS-SiO₂ NCs.

Spectroscopy analysis

The UV-Vis spectroscopy measurements of all synthesized QDs samples were recorded on Cary 5000 (UV-Vis-NIR spectrophotometer, Varian, Australia) in the wavelength ranging from 400 to 800 nm. PL was collected by Cary Eclipse spectrofluorometer (Varian, Australia). All Spectroscopic measurements were performed at room temperature.

Transmission electron microscope (TEM)

High-resolution transmission electron microscope (HR-TEM, Tecnai G20, FEI, Netherland) was used for imaging. A drop of a dilute sample solution deposited on an amorphous carbon coated-copper grid. Bright field imaging mode was performed using Eagle CCD camera at electron accelerating voltage 200 kV using lanthanum hexaboride (LaB6) electron source gun.

Dynamic light scattering

Dynamic light scattering (DLS) measurements were performed using the Zetasizer nano-ZS equipped with 633 nm laser (Malvern Instruments Ltd, UK). The analysis yields the size distribution of the particles inside the sample and polydispersity index. The hydrodynamic particle diameter is available via the

Stokes-Einstein equation. To transfer the weighted hydrodynamic particle sizes distribution to number %, a Mie correction is used to consider the size-dependent extinction coefficient (Finsy and De Jaeger, 1991). Each run was replicated three times to ensure data consistency.

X-ray diffraction analysis

All synthesized NCs samples were dried and the X-ray diffraction (XRD) patterns of the dry powder of each sample were obtained starting from $2\theta = 4^\circ$ to 80° in a continuous scan mode in steps of 0.02° via Philips Panalytical X'pert Pro X-ray diffractometer using Cu Ka (1.54059 \AA) radiation, and X-ray generator operating at 45 kV and 30 mA.

Biological evaluation

Cell culture

Liver hepatocellular carcinoma (HepG2) cells were obtained from the Egyptian Organization for Biological Products and Vaccines (VACSERA). Cells were cultured in RPMI-1640 media supplemented with 10% FBS and then incubated in 5% CO_2 at 37°C .

Mitochondrial activity

For assessing the cytotoxicity effect of Si-CdSe/ZnS NCs on HepG2 cells, the cell proliferation reagent WST-1 was used to evaluate the mitochondrial activity (Pardo *et al.*, 2017). Briefly, 5×10^4 cell/well were loaded in a 96-well plate 18 h after seeding, the old media was removed and new media containing CdSe/ZnS-SiO₂ NCs with different concentrations ranging from 5.56-50.04 nM cadmium. Cells incubated with media free of QDs were used as negative controls and cells incubated with media contain uncoated CdSe/ZnS NCs were used as positive controls. WST-1 kit reagent was added 4 h prior to completion of the incubation period. The absorption of samples was measured by microtiter reader (Tecan, Austria) at 450 nm. Experiment was performed in triplet manner.

Alkaline comet assay

According to Tice and Vasquez, the purpose of this protocol is to detect DNA damage in eukaryote cells (Tice and Vasquez, 1999). Standard microscopic slides were dipped into hot 1.0% normal melting point agarose, and the bottom of the slides was cleaned to remove excess agarose. Ten μl aliquot of control and treated HepG2 cells suspended in cold mincing solution HBSS with 20 mM EDTA, 10% DMSO, were mixed with 75 μl of 0.5% LMA and were added to the precoated slides. After solidification, slides were placed in a cold fresh lysing solution for 24 h at 4°C in the dark. Subsequently, the slides were incubated in freshly-made alkaline buffer (pH > 13) for 20 min. Electrophoresis was performed at 300 mA and 25 V for 20 mi, then the alkali was neutralized with 0.4 M Tris (pH 7.5), fixed in 100% cold ethanol and air dried. After the complete drying, DNA was stained with ethidium bromide (2 mg/ml). Finally, about 50 images were randomly acquired for every sample using a fluorescence microscope and analyzed for: The Tail Moment, tail length, and % DNA in the tail using Comet Assay IV software (Perceptive Instruments, Suffolk, UK).

Confocal Laser Scanning Microscopy (CLSM)

Images for HepG2 cells were captured after the incubation with CdSe/ZnS-SiO₂ NCs using confocal laser scanning microscope (CLSM, LSM 710, Carl Zeiss, Germany) supported with Zen2009 software and equipped with CO₂ incubator. Processing was done using Zen2012 (blue edition). Specimens were excited using the 488 nm laser line of an Argon laser. Oil immersion objective 40 \times was used to obtain images.

Cellular localization study using CdSe/ZnS-SiO₂ QDs by Confocal Laser Scanning Microscopy (CLSM)

To study localization of CdSe/ZnS-SiO₂ NCs in mitochondria, CellLight® Mitochondria-RFP*BacMam 2.0 (molecular probes by life technologies, USA) was used Analogous to Saulite description (Saulite *et al.*, 2017), and according to the manufacturer's recommendation. Briefly, 2 ml RPMI media containing 2 μL of Mitochondria-RFP was added to 10.000 HepG2 cells attached in glass-based Petridish, incubated overnight. Cells were stained with 4',6-diamidino-2-phenylindole (DAPI) as a counter stain for nucleus. CdSe/ZnS-SiO₂ NCs were added immediately before the start of images acquisition using CLSM. To study localization of CdSe/ZnS-SiO₂ NCs in Lysosomes, CellLight® Lysosomes-RFP*BacMam 2.0 (molecular probes by life technologies, USA) was used following the same procedure in a separate Petri dishes.

Live cell imaging by confocal laser scanning

Microscopy (CLSM). Cellular internalization efficiency of the prepared NCs in HepG2 cells was estimated by live cell imaging. HepG2 cells were cultured on glass-based Petridish and exposed to CdSe/ZnS-SiO₂ NCs at concentrations of 5.56 nM. Cells were incubated in 37°C with 5% CO_2 . Time series experiments of live cells were performed for 8 h starting immediately after adding the CdSe/ZnS-SiO₂ NCs. Images were captured every 30 minutes by using 0.2% of 488 nm laser line.

Statistical analysis

Cell survival and DNA damage were expressed as the mean \pm standard error (SE) and the significance of the differences, compared with control, was calculated using Graph pad prism 7.00. $P < 0.05$ were considered statistically significant according to Student's A nova-test.

RESULTS AND DISCUSSION

Characterizations of CdSe QDs

The absorption spectra of a series of CdSe QDs were taken during synthesis process after different growth time ranged from 2-15 min (Figure 1). Results showed relatively sharp absorption feature near the absorption onset that corresponds to the excitonic peak. As the excitonic peak position depends on the particle size, its form and width are shaped by the pattern of size distribution. Consequently, due to quantum confinement, the increase of particle size resulted in a bathochromic (red) shift of the absorption onset (Hines and Kamat, 2014).

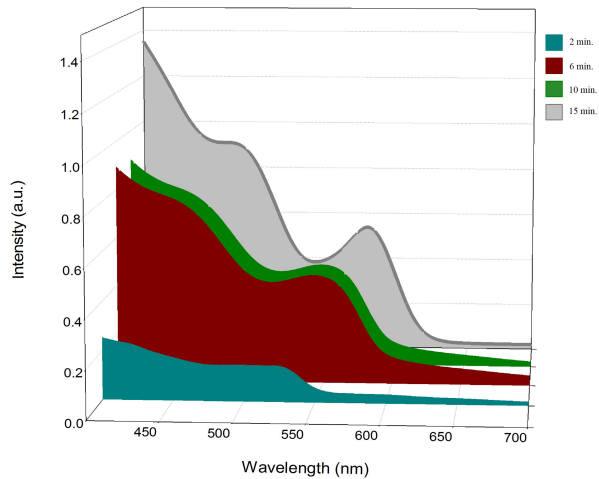


Fig. 1: The absorption spectra of the CdSe nanocrystals. Monitoring the change in the absorption as a function of growth time UV-Vis absorption spectra were recorded in the range from 400 to 700 nm to CdSe QDs aliquots during synthesis process at different growth time (from 2 to 15 minutes).

XRD pattern showed that, the core NCs was very well matching with the cubic zinc blende structure “JCPDS 01-088-2346”. While, core/shell had the same pattern of the core plus additional peaks of cubic ZnS with zinc blende structure “JCPDS 00-065-0722”. In addition, core/shell-coated with silica showed the same previous peaks of core and core/shell plus additional peaks of tetragonal CdSe/ZnS-SiO₂ structure “JCPDS 01-073-3435”. As shown in (Figure 2, a), the broadening of the XRD pattern peaks indicates the small particle (crystallite) size to the nanometric size (Iranmanesh *et al.*, 2015). This agrees with the TEM images of the CdSe, CdSe/ZnS core/shell and CdSe/ZnS-SiO₂ NCs (Figure 2, b), which illustrate that most particles have a homogeneous spherical shape and size with an average diameter of about 2, 2.5, 35 nm, respectively.

Further characterizations were performed to the three prepared samples CdSe, CdSe/ZnS and CdSe/ZnS-SiO₂. The optical UV-Vis absorption and PL spectra of CdSe (Figure 3) showed an excitonic absorption at 532 nm and PL spectrum maximum emission around 548 nm, while the DLS analysis of the core sample showed a hydrodynamic diameter of 6.5 nm. On the other hand, the absorption spectrum of CdSe/ZnS QDs showed 7 nm bathochromic shift to give a maximum excitonic absorption at 530 nm (Figure 4). Also, PL maximum emission after the addition of ZnS shell were at 553 nm. While the hydrodynamic diameter obtained from DLS showed 7.1 nm size. Whereas absorption spectrum of CdSe/ZnS-SiO₂ NCs showed that, the SiO₂ coating causes relatively broadening of the excitonic peak which influenced by the distribution in size (Figure 5). In addition, CdSe/ZnS-SiO₂ PL emission maximum located at 577 nm, with 29 nm bathochromic shift respectively relative to the core. While CdSe/ZnS-SiO₂ sample exhibited size distribution peak around 104 nm according to DLS analysis. The polydispersity index (PDI) values of all samples were typically >0.5 that distinctly ensure particles size and shape homogeneity (Bhattacharjee, 2016). The size distribution of NCs obtained from DLS analysis was slightly larger than the equivalent size appeared in TEM images; this can be explained depending on the difference between the applied techniques of each system. Whereas DLS sizes arise from the calculated hydrodynamic diameter depending on the intensity of the scattered laser from the sample’s particles (Fischer and Schmidt, 2016), the TEM sizes arise from the investigation of the sample by transmitted electron beam, that gives a more real result about the particles size and shape. The difference between the sizes obtained from both techniques reached its maximum in the case of the CdSe/ZnS-SiO₂ sample, this could be explained by the aggregation of the particles, which make a confusion for the detector that could not distinguish between scattered light from one large particle, or numerous aggregated small particles.

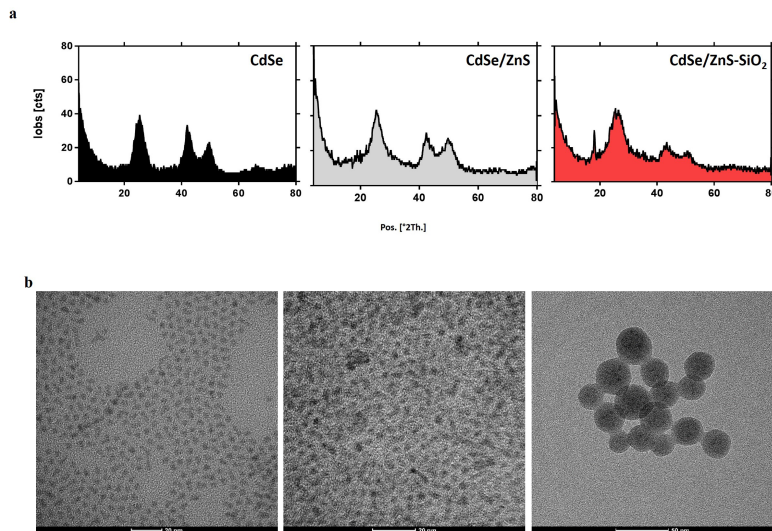


Fig. 2: XRD and TEM characterizations of core, core/shell and core/shell-coated NCs. (a) XRD pattern for the CdSe core, CdSe/ZnS core/shell and CdSe/ZnS-SiO₂ core/shell-coated NCs, showing the corresponding miller indices of diffraction planes. (b) TEM images for CdSe, CdSe/ZnS and CdSe/ZnS-SiO₂ NCs, respectively from left to right. (Scale bars 20, 20, 50 nm respectively).

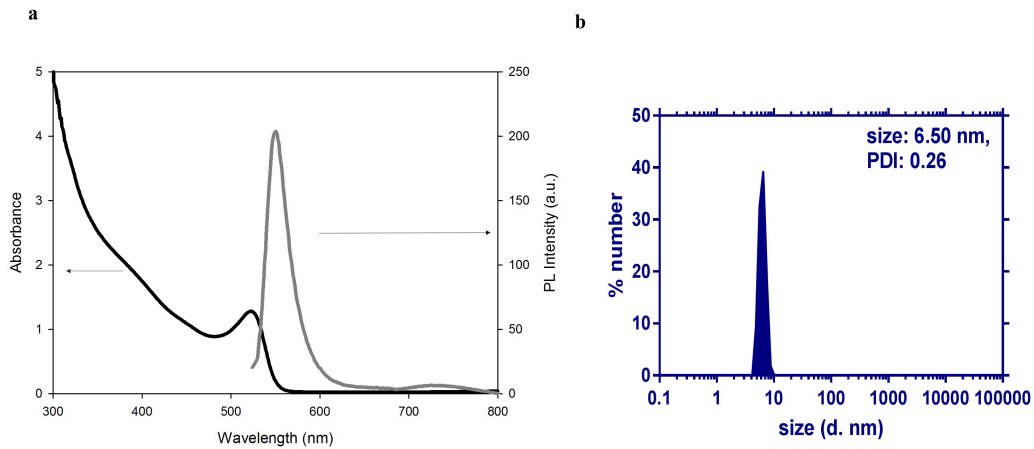


Fig. 3: PL spectra and size distribution of CdSe core. (a) UV-Vis absorption and PL spectra and size distribution of the as-prepared CdSe, (b) Show particle size distribution of CdSe.

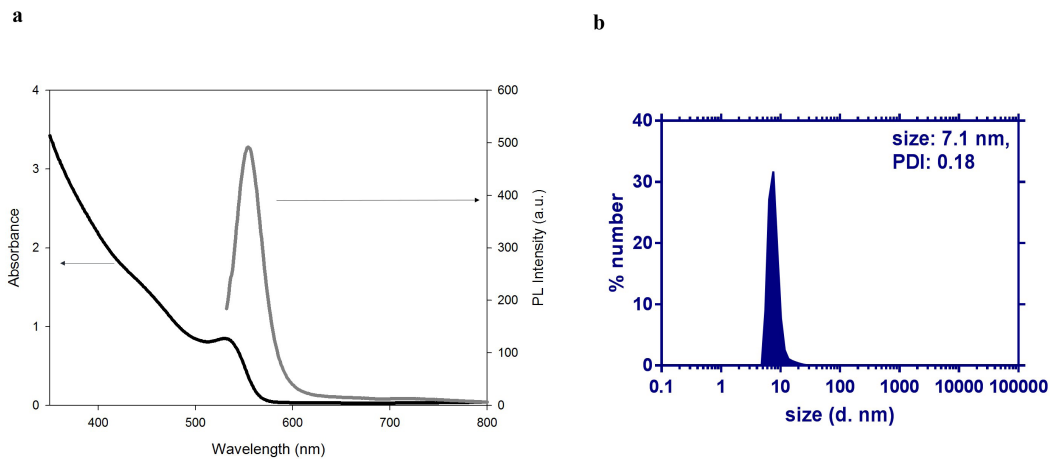


Fig. 4: PL spectra and size distribution of CdSe/ZnS core/shell. (a) UV-Vis absorption and PL spectra and size distribution of the as-prepared CdSe/ZnS, (b) particle size distribution of CdSe/ZnS.

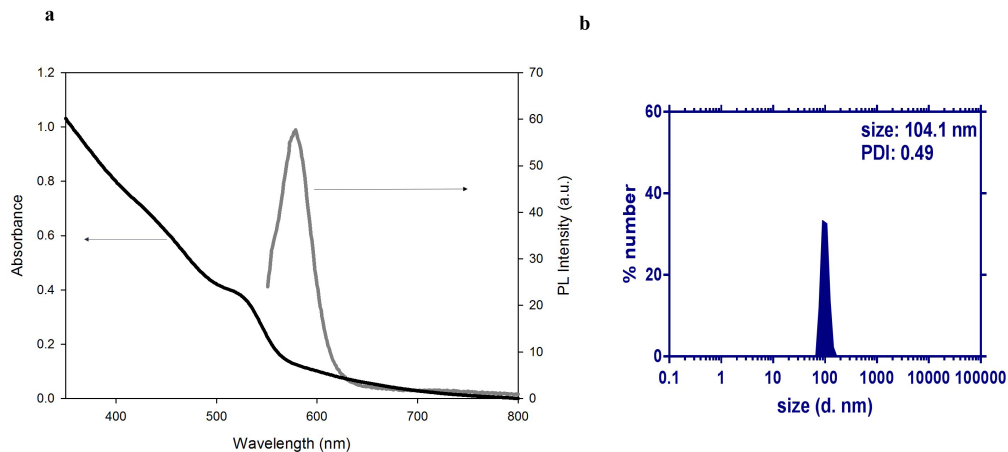


Fig. 5: PL spectra and size distribution of CdSe/ZnS-SiO₂ core/shell-coated NCs. (a) UV-Vis absorption and PL spectra and size distribution of the as-prepared CdSe/ZnS-SiO₂, (b) particle size distribution of CdSe/ZnS-SiO₂.

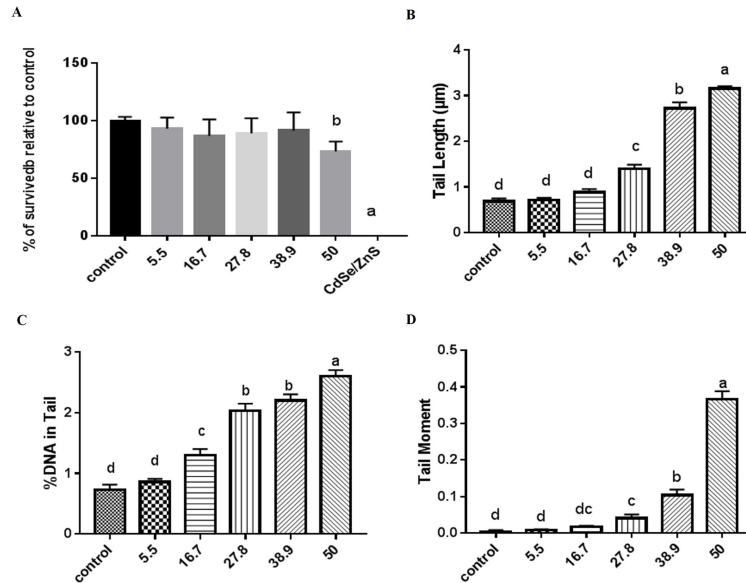


Fig. 6: Biological evaluation of core/shell-coated NCs. (a) survival % relative to controls for HepG2 cell line. After exposure to different concentrations of CdSe/ZnS-SiO₂ NCs. Error bars represent standard error from three different experiments. (b) DNA damage represented as tail length (μm), (c) % DNA in tail and (d) tail moment in different treatment groups in HepG2 cells. X axis represents QDs concentration by μM. Results are expressed as mean ± SE, significant difference with negative control using T test, bars denoted by the same letter(s) are not statistically different at P < 0.05 according to Student's A nova-test.

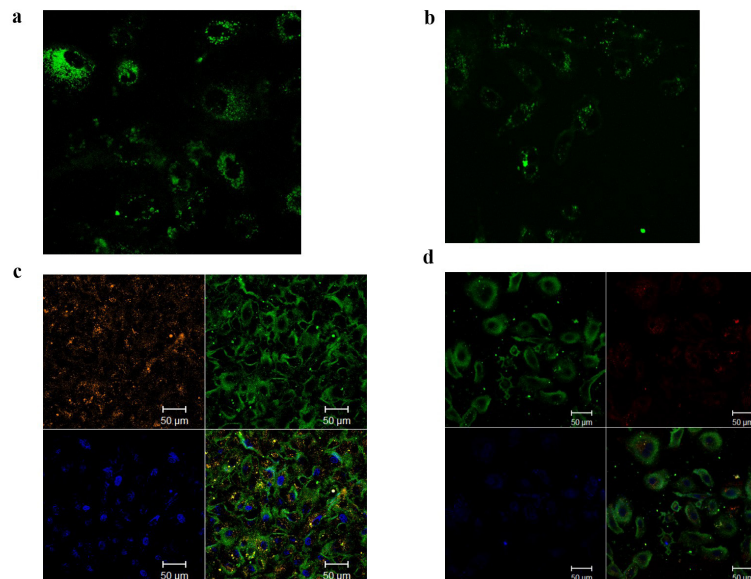


Fig. 7: CLSM imaging of HepG2 cells. (a) Cells stained with CdSe/ZnS-SiO₂ only, (b) Cells stained with CdSe/ZnS-SiO₂, lysosomes-RFP and DAPI, (c) Cells stained with CdSe/ZnS-SiO₂, Mitochondria-RFP and DAPI. Pseudocolors green, red, orange and blue indicate the fluorescence from the NCs, mitochondria, lysosomes, and nucleus, respectively.

Biological evaluation of NCs effect

Based on the results of the cytotoxicity studies performed by applying different concentrations of CdSe/ZnS-SiO₂ (Figure 6 a), it could be confirmed that the prepared NCs possess good biocompatibility up to 40 nM (no significant reduction in HepG2 cells growth relative to control). While, with increasing the concentration of NCs to 50 nM, it showed low toxicity. Five nM of CdSe/ZnS at ODE was used as a negative control, which show 100% lethal effect.

The statistical significant increased (P < 0.05) in DNA damage as assessed by tail length, percentage of the DNA in tail and tail moment, indicated that the administration of CdSe/ZnS-SiO₂ at 5.5 and 16.7 μM doesn't induce significant DNA damage when compared with control group of HepG2 cells (cells without any NCs, Figures 6, c, d). While, all other higher concentrations showed a statistically significant increase of all DNA damage parameters in comparison with the HepG2 cells control group (P < 0.05).

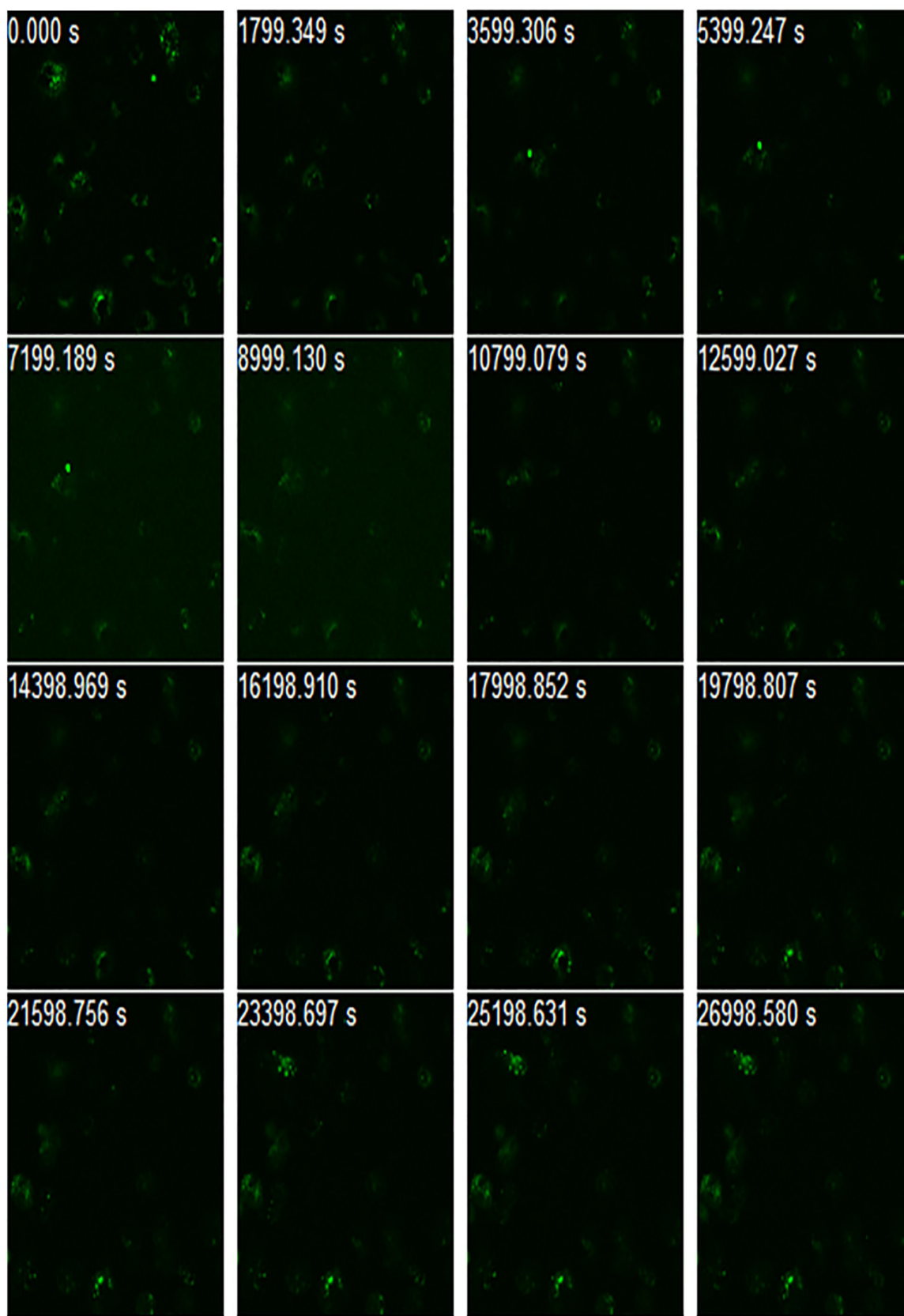


Fig. 8: Confocal Laser Scanning microscopy images of live HepG2 cell. HepG 2 cell line incubated with CdSe/ZnS-SiO₂ by and continuous imaging was acquired by time lapse mode for 8 hours.

According to Tsoi's findings, we can attribute the DNA damage to the cadmium core of QDs that could generate free radical species in the surrounding media (Tsoi *et al.*, 2013).

On the other hand, The CLSM micrographs (Figures 7 a, b) confirmed the internalization of QDs in the cytoplasm including mitochondria and lysosomes. However, it showed no internalization inside the nucleus. These results agree with the finding of prior works (Deerinck, 2009; Xiao *et al.*, 2010). Cellular localization of CdSe/ZnS-SiO₂ QDs in HepG2 cells was tested using CLSM. By imaging HepG2 cells pre-incubated over night with Mitochondria-RFP/lysosomes-RFP and 30 min with DAPI, after seconds of adding CdSe/ZnS-SiO₂ NCs (Figures 7 c, d).

Live cell imaging of the prepared NCs in HepG2 cells showed that, cellular uptake of the prepared NCs was very fast as CdSe/ZnS-SiO₂ NCs was inside the cells from the first minute of the experiment time (Figure 8). Also, signal from CdSe/ZnS-SiO₂ NCs showed no decay or photobleaching, what ensure its stability inside the cell up to eight hours.

CONCLUSION

These results confirmed the effective role of silicon as surface coating of CdSe/ZnS NCs. Rather than the role of CdSe/ZnS-SiO₂ in labeling and imaging of cancer cells due to their good fluorescence emission inside the cytoplasm, non-toxicity at low concentrations and their fast uptake that could be due to the silica shell that help in the internalization of the NCs throw the cells membrane. However, staining cell's nucleus still a challenge as it needs further surface modification.

CONFLICT OF INTERESTS

There are no conflicts of interest.

REFERENCES

- Bhattacharjee S. DLS and zeta potential - What they are and what they are not? *Journal of Controlled Release*, 2016; 235:337–351.
- Cui H, Song W, Cao Z, Lu J. Simultaneous and sensitive detection of dual DNA targets via quantum dot-assembled amplification labels. *Luminescence*, 2016; 31:281–287.
- Deerinck TJ. The Application of Fluorescent Quantum Dots to Confocal, Multiphoton, and Electron Microscopic Imaging. *Imaging*, 2009; 36:112–116.
- Dhawan A, Sharma V. Toxicity assessment of nanomaterials : methods and challenges. *Anal Bioanal Chem*, 2010; 398:589–605.
- Finsy R, De Jaeger N. Particle Sizing by Photon Correlation Spectroscopy. Part II: Average values. *Particle & Particle Systems Characterization*, 1991; 8:187–193.
- Fischer K, Schmidt M. Pitfalls and novel applications of particle sizing by dynamic light scattering. *Biomaterials*, 2016; 98:79–91.
- Hines DA, Kamat PV. Recent Advances in Quantum Dot Surface Chemistry. *ACS Applied Materials & Interfaces*, 2014; 6:3041–3057.
- Hoshino A, Hanada S, Yamamoto K. Toxicity of nanocrystal quantum dots: The relevance of surface modifications. *Archives of Toxicology*, 2011; 85:707–720.
- Ibrahim SA, Ahmed W, Youssef T. Photoluminescence and photostability investigations of biocompatible semiconductor nanocrystals

coated with glutathione using low laser power. *Journal of Nanoparticle Research*, 2014; 16:6.

Iranmanesh P, Saeednia S, Nourzpoor M. Characterization of ZnS nanoparticles synthesized by co-precipitation method. *Chin Phys B*, 2015; 24:1–4.

Kim J, Biondi MJ, Feld JJ, Chan CW. Clinical Validation of Quantum Dot Barcode Diagnostic Technology. *ACS Nano*, 2016; 10:4742–4753.

Liu F, Ye W, Wang J, Song F, Cheng Y, Zhang B. Parallel comparative studies on toxicity of quantum dots synthesized and surface engineered with different methods in vitro and in vivo. *International Journal of Nanomedicine*, 2017; 12:5135–5148.

Massey M, Wu M, Conroy E M, Algar W R. Mind your P's and Q's: the coming of age of semiconducting polymer dots and semiconductor quantum dots in biological applications. *Current Opinion in Biotechnology*, 2015; 34:30–40.

Medintz I, Hildebrandt N. 2014. FRET – Förster Resonance Energy Transfer From Theory to Applications. Wiley-VCH.

Oh E, Liu R, Nel A, Gemill K B, Bilal M, Cohen Y, Medintz IL. Meta-analysis of cellular toxicity for cadmium-containing quantum dots. *Nature Nanotechnology*, 2016; 11:479–486.

Pardo M, Katra I, Schaeur JJ, Rudich Y. Mitochondria-mediated oxidative stress induced by desert dust in rat alveolar macrophages. *Geo-Health*, 2017; 1:4–16.

Peng ZA, Peng X. Formation of high-quality CdTe, CdSe, and CdS nanocrystals using CdO as precursor. *Journal of the American Chemical Society*, 2001; 123:183–184.

Peuschel H, Ruckelshausen T, Kiefer S, Silina Y, Kraegeloh A. Penetration of CdSe/ZnS quantum dots into differentiated vs undifferentiated Caco-2 cells. *Journal of Nanobiotechnology*, 2016; 14:1–19.

Saulite L, Dapkute D, Pleiko K, Popena I, Steponkiene S, Rotomskis R, Riekstina U. Nano-engineered skin mesenchymal stem cells: potential vehicles for tumour-targeted quantum-dot delivery. *Beilstein Journal of Nanotechnology*, 2017; 8:1218–1230.

Thomas JA. Optical imaging probes for biomolecules: an introductory perspective. *Chem. Soc. Rev*, 2015; 44:4494–4500.

Tice R, Vasquez M. pH > 13 alkaline single cell gel (SCG) assay to the detection of DNA damage in mammalian cells, 1999; 1995:184–191.

Tsoi K, Dai Q, Alman B, Chan W. Are Quantum Dots Toxic? Exploring the Discrepancy Between Cell Culture and Animal Studies. *Accounts of Chemical Research*, 2013; 46:662–671.

Vibin M, Vinayakan R, John A, Fernandez F, Abraham A. Effective cellular internalization of silica-coated {CdSe} quantum dots for high contrast cancer imaging and labelling applications. *Cancer Nanotechnology*, 2014; 5:1–12.

Xiao Y, Forry S, Gao X, Holbrook R, Telford W, Tona A. Dynamics and mechanisms of quantum dot nanoparticle cellular uptake. *Journal of Nanobiotechnology*, 2010; 8:13.

How to cite this article:

ElZorkany HE, El-Shorbagy HM, Farroh KY, Youssef T, Sabet S, Salaheldin TA. Monitoring the cellular uptake of Silica-Coated CdSe/ZnS quantum dots by Time lapse Confocal Laser Scanning Microscopy. *J App Pharm Sci*, 2018; 8(03): 001-008.